International Journal of Engineering

Journal Homepage: www.ije.ir

A Study on the Contact Ellipse and the Contact Pressure During the Wheel Wear through Passing the Tracks including Several Sharp Curves

S. M. Salehi, G. H. Farrahi*, S. Sohrabpour

School of Mechanical Engineering, Sharif University of Technology, Tehran, Iran

PAPER INFO

Paper history:
Received 19 December 2017
Received in revised form 11 February 2018
Accepted 19 February 2018

Keywords:
Wheel Wear
Maintenance Technique
Sharp Curved Railways
Empirical Study
Wheel Flange Wear
Wheel Longevity Enhancement

ABSTRACT

Wheel wear has been a concern in the railway for several decades. Studying the form change of the wheel/rail contacts in particular railways consisting of sharp curves helps to identify the risk of severe or catastrophic wear to minimize maintenance costs in order to be competitive in the transportation business. In this paper, the wheel/rail contact was studied on the particular railways. The experimental measurement of wheel profiles was used as an input to Hertz Contact Theory (HCT). It was found that: 1) for these railways the wheel flange is highly worn; 2) a 5th order polynomial function is appropriate to model the wear behavior of the critical wheel; 3) the minimum and maximum contact ellipse surface areas occur in Sd=22.29 *mm* and Sd=32 *mm*, respectively; 4) the maximum and minimum surface areas of the contact ellipse occur at points in which the contact pressure are minimum and maximum, respectively; and finally 5) the flange thickness region between 25 to 29 *mm* can be chosen as an appropriate range for the wheel maintenance purposes.

***doi**: 10.5829/ije.2018.31.05b.19*

1. INTRODUCTION

Wheel wear in tracks has been a concern in the railway business for several decades. In the contact of wheel/rail the wheel flange and tread are the subject of wear. Although rail/wheel lubrication considerably decreases the wear rate, still wear is considerably great especially in sharp curves [1, 2]. Studying the form change of the wheel/rail contacts in particular railways consisting of sharp curves can help to identify the risk of severe or catastrophic wear resulting from increased train speeds and axle loads [3]; also, it can help in determining more efficient maintenance schedules for track and wagons [4, 5]. Furthermore, wheel flange wear is a major factor in the maintenance costs of mentioned railways. It would be minimized in order to enable the railway system to compete with the other modes (e.g. road and airway) of the transportation business [1, 6].

The wheel/rail wear has been extensively studied. The important experimental researches have been reviewed by Clayton [7], Lewis and Olofsson [8], Enblom [9], Sheinman [10], Neil [11], Zacher [12] and others. Some of the experimental studies have been conducted through laboratory tests. Others based on experience and measurements on in-service vehicles and track (field experiments) [13-15]. The difficulties and expenses involved in field experiments force researchers to use, whenever possible, the laboratory tests and simulations [1].

The analytical method of HCT was published in 1881 and extensively applied in many engineering fields which deal with contact problems to calculate normal and tangential contact stresses [16-18]. This theory has been used in recent works such as investigating the growth of shell-type defects in the head of a railroad [19, 20], fatigue life model to describe the damage of wheels [21], three-dimensional (3D) rail-fatigue model PHOENIX to describe the fatigue initiation in rail subsurface [16]. Yan and Fisher [16] examined the practicability of the HCT in wheel-rail interaction and emphasized that several 3D FE investigations have been performed for real rail/ wheel/ sleeper/ bedding configurations. The numerical results from the 3D FE calculations have been compared to the HCT. Their

*Corresponding Author Email: *farrahi@sharif.edu* (G. H.Farrahi)

Please cite this article as: S. M. Salehi, G. H. Farrahi, S. Sohrabpour, A Study on the Contact Ellipse and the Contact Pressure During the Wheel Wear through Passing the Tracks including Several Sharp Curves, International Journal of Engineering (IJE),IJE TRANSACTIONS B: Applications Vol. 31, No. 5, (May 2018) 826-833

comparisons showed that the error of the plasticization is mostly less than 10 percents which is acceptable in practical engineering problems in comparison to the highly simplification of the problem.

This study is about wheel/rail contact in railways consisting several sharp curves using the experimental measurements of wheel profiles as input and the analytical approach based on HCT [22]. The contact point position and stresses are calculated in the contact area from the empirical measurements of wheel profile until the wheel detachment [23-25]. The result of this study will be of value to the engineering estimation, analysis, design and maintenance aspects of railway systems involving sharp curved tracks. Moreover, this approach could be a commence to develop procedures in order to relate the wheel-rail contact characteristics during curving to the rate of flange wear. This would requires a more sophisticated calculation of contact properties (including relevant wheelset position, multi-Hertzian contacts, creepages/forces, etc.) and wear calculation/modelling. Further benefit of future developments of this work for the rolling stock maintainers is the consideration of the amount of material to be removed during re-profiling of the wheels to restore a full wheel profile (so-called Economic Tyre Turning).

2. MATERIALS AND METHODS

2. 1. Experimental Measurements

2. 1. 1. The Railway, Wagon and Wheels The case that this study mainly focuses on is the "Southern line" of Iran which is the largest and most significant rail line to transport passenger and freight from Iran's capital, Tehran, to three important transit ports: "Imam Khomeini", "Mahshahr", and "Khorramshahr". This path was selected since a high rate of wheel flange wear occurs which leads to a significant reduction of wheel life. A wagon of the "Plure Sabz" train with type MD523 bogies with a weight of 60 tons was chosen which has 8 wheels with the S1002 standard profile (Figure 1). Different materials are used in wheels and rails.

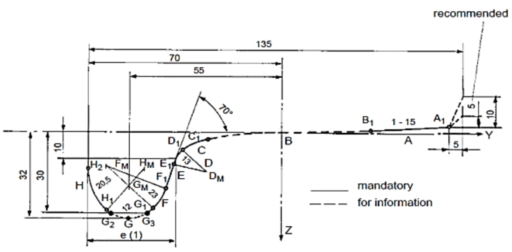

Figure 1. The standard S1002 profile for wheels with a flange height of 30 mm [26]

The material of the rail is considerably harder due to prevent the rail wear while the wheels are worn subjected to various kinds of loads and stresses when they come in contact with track. A steel rail has a flat bottom and its cross section is derived from an I-profile. The upper flanges of the I-profile have been converted to form the rail head. According to UIC510-2 [26], the wagon detachment is necessary, in order to reprofile or replace the worn wheels, when the thickness of the wheel flange is reduced to 22 *mm*.

2. 1. 2. Measurements and Data Processing The manual compound caliper and the automatic laser view are the mostly used devices in order to record the profiles of wheels. In this work the laser view was used to record the worn profiles of the wheels (Figure 2). The measurements are performed in each round trip of the in-service wagon with new installed wheels until the wheels flange thicknesses (Sd) reach the limit of 22 *mm*. "least-squares-method" curve fitting techniques are used to express the mathematical relationships between the Sd parameter and the wheel's traveled distance. Polynomial functions from the first order (linear) to higher orders were evaluated since the desired accuracy of the results was achieved:

$$y = a_n x^n + a_{n-1} x^{n-1} + \cdots + a_2 x^2 + a_1 x + a_0 \quad (1)$$

The least squares method minimizes the summed square of residuals to approximate the coefficients. The residual for the*i*th data point r_i is defined as a difference between the observed response value y_i and the fitted response value $\hat{y}_i$ as:

$$r_i = y_i - \hat{y}_i \quad (2)$$

$$S = \sum_{i=1}^{n} r_i^2 = \sum_{i=1}^{n} (y_i - \hat{y}_i)^2 \quad (3)$$

2. 1. 3. Contact Point When two rigid bodies (wheel and rail) are pressed against each other by a normal force, a contact region is formed at the point at which they contact each other. The contact points are determined using the measured profiles of rail and wheel. Figure 3(a) shows the standard wheel profile of S1002 which is utilized in Iran's railway system with an initial flange height of 30 mm [26].

Figure 2. The laser view instrument (indicated by arrows) to measure the wheel profiles

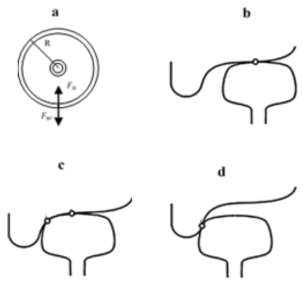

Figure 3. (a) Wheel and rail contact in a side view, **(b)** One point thread contact, **(c)** two point thread/flange contact, and **(c)** One point thread contact [27]

Through the measurements, it was found that the contact point is located at zone B when considering the contact point in the straight track. The mathematical equation of the zone B is [26]:

$$\begin{aligned} Z = {} & 0 - 3.358537058\times10^{(-2)}y + 1.565681624\times10^{(-3)}y^2 \\ & - 2.810427944\times10^{(-5)}y^3 + 5.844240864\times10^{(-8)}y^4 \\ & - 1.562379023\times10^{(-8)}y^5 + 5.309217349\times10^{(-15)}y^6 \\ & - 5.957839843\times10^{(-12)}y^7 + 2.646656573\times10^{(-13)}y^8 \end{aligned} \tag{4}$$

Using the wheel profile equation in the zone B, the transverse curvature (*R)* of the wheel is obtained by:

$$R = \frac{(1+\dot{y}^2)^{\frac{3}{2}}}{\ddot{y}} \tag{5}$$

where $\dot{y}$ and $\ddot{y}$ are the first and second derivatives of the transverse dimension of the wheel (y).

Calculations show the value of 320 mm for the S1002 standard profile in contact with the UIC60 profile of the rail. The sign of the curvature is negative when the center of the curvature is outward with respect to the wheel center (concave) [16].

2. 2. Hertz Contact Theory (HCT) Some references used initial theories of elasticity which specifically concerned with the calculation of railway rail/wheel surface tractions. HCT assumes that: 1) the contact surfaces are smooth; 2) the contact between elastic bodies should be frictionless; 3) the contact is assumed to be elliptical in shape; and 4) the significant dimensions of the contact area should be much smaller than the dimensions and the radii of curvature of the bodies in contact [4, 16]. However, due to the simplicity of the estimations, many researchers use Hertzian theory in various ways to model non-Hertzian contacts or using the model as a tool to assist in the making of operational or maintenance decisions or design changes such as rail or wheel profile optimization [16].

The shape and size of the contact region between two elastic bodies in static contact are given by Hertz's static solution. If the wheel and rail are composed of two different materials, a semi-ellipsoid distribution of the pressure could be obtained as:

$$P = P_m\left(1 - \frac{x^2}{a^2} - \frac{y^2}{b^2}\right); \quad |x| \le a, |y| \le b \tag{6}$$

where, the *x*- and *y*- axes extend along the ellipse's major (a) and minor (b) semi-axes, respectively. The origin of the coordinate system is located at the contact center and the p_m is the largest contact pressure, which appears at the contact center obtaining from the external normal compressive force to the contact region *F*:

$$P_{max} = \frac{3F}{2\pi ab} \tag{7}$$

To calculate the contact pressure *P*, and the ellipse's semi axes *a* and *b*, the parameters *A* and *B* are first defined as:

$$A = \frac{1}{R_1} + \frac{1}{R_2} \tag{8}$$

$$B = \frac{1}{R_1'} + \frac{1}{R_2'} \tag{9}$$

where R_1 and R_2 are the principal rolling radii of the wheel and rail, and R_1' and R_2' are the principal transverse radii of curvature of the wheel and rail profiles at contact point, respectively (Figure 4).
The ellipse's semi-axes *a* and *b* are obtained from:

$$a = m\left(\frac{3F(\delta_1+\delta_2)}{A+B}\right)^{\frac{1}{8}} \tag{10}$$

$$b = n\left(\frac{3F(\delta_1+\delta_2)}{A+B}\right)^{\frac{1}{8}} \tag{11}$$

where, δ_1 and δ_2 are parameters related to the wheel and rail materials calculated from:

$$\delta_1 = \frac{1-\nu_1^2}{2E_1} \tag{12}$$

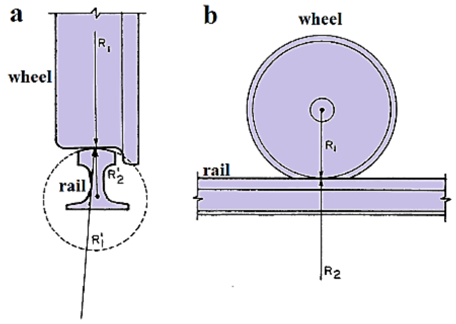

Figure 4. Principal radii of curvatures of the **(a)** rail and **(b)** wheel

$$\delta_2 = \frac{1-\nu_2^{\,2}}{2E_2} \tag{13}$$

where, ν_1 and ν_2 are Poisson's ratios for the wheel and rail materials, respectively. E_1, E_2 are Young's moduli of elasticity of the wheel and rail materials, respectively. The coefficients m and n in Equations (10) and (11) are obtained from the Table 1 with respect to β angle defined as:

$$\cos\beta = \frac{A-B}{A+B} \tag{14}$$

The calculations were conducted for each profile using the presented following procedure. The transverse radius of curvature of the wheel profile varied due to wear and needed to be calculated.

Table 2 represents the mechanical parameters of the wheel and rail and the wheel loading as well as the curvature radii which are used to the calculations. Even though the contact interface between the wheel and the surface is initially a single point (Figures 3(a) and 3(b)), the contact interface will grow to become a surface as the wheel deforms and wears. In addition, the contact area in curves varies into a two point contact condition; where, the stresses and loads are mostly involved in the flange of wheel (Figure 3(c)) or only exerted on the flange (Figure 3(d)). In this work, it is observed more wear occurs in the flange area of the wheels due to passing through many curves along the railway. However, the analysis is performed for the selected wheel (the critical wheel) when it is on the straight part of the track (but not in the curved track) until the limit of Sd=22 mm is reached (the detachment of wheel) according to UIC standard [28]. Hence, the analysis is based on one point contact geometries. The critical wheel is the first wheel which reaches the flange thickness limit ($sd \approx 22\ mm$).

TABLE 1. Parameters m and n with respect to β angle [28]

$\boldsymbol{\beta}$	$\boldsymbol{m}$	$\boldsymbol{n}$
90	1	1
80	1.128	0.893
70	1.284	0.802
60	1.486	0.717
50	1.754	0.641
40	2.136	0.567
30	2.731	0.493
20	2.778	0.408
10	6.612	0.319
5	11.236	0.2969

TABLE 2. Wheel and rail parameters for the calculations of the HCT

Parameters	**Value**
Elasticity Module of Wheel E_1	206 *GPa*
Elasticity Module of Rail E_2	210 *GPa*
Wheel load F	78200 *N*
Poisson Coefficient of Wheel ν_1	0.27
Poisson Coefficient of Rail ν_2	0.3
Wheel Longitudinal Radius R_1	460 *mm*
Rail Longitudinal Radius R_2	∞
Wheel transverse Radius R'_1	Is calculated For each profile (*mm*)
Rail transverse Radius R'_2	300 *mm*

3. RESULTS AND DISCUSSIONS

In this section the experimental results of wheel flange wear, in particular railway "the Southern line" of Iran, are presented and discussed. Afterwards, HCT is also used to calculate the contact ellipse diameters in the longitudinal and lateral directions and the semi-ellipsoid distribution of the pressure (or normal stress distribution). Although the friction is important to the wheel and rail contact area through the tangential forces which appearing in the wear of wheel, our procedure implicitly considers the friction effects on wheel during the wear process by measuring the profiles in a systematic experimental data record.

3. 1. Wheel Wear Behavior

Figure 5 shows the new wheel profile corresponding to the S1002 standard profile with Sd=32 *mm* and the final worn profile of the wheel corresponding to the Sd=22.29 *mm* for the critical wheel of the wagon. It can be found that the severe wheel flange wear was occurred and the wheel tread wear is very small in comparison to the wheel flange wear.

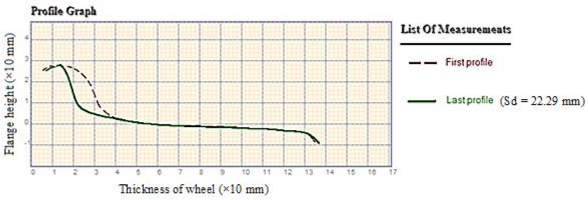

	Measurement	Maintenance	FRA	AAR
Flange Height	28.65	38.10	38.10	38.10
Flange Thickness	22.29	23.81	23.81	23.81
Rim Thickness	35.41	22.23	22.23	22.23
Tread Hollow	0.00	1.59	1.59	1.59

Figure 5. The new (red) and the last worn (green) profiles of the critical wheel (all parameters are in mm). The worn profile shows the severe wheel flange wear in the Southern line of Iran

As mentioned in sections 1 and 2, this is the most important characteristic of the railways including many curves such as the considering railway of "Southern line of Iran". These curves cause a two-point contact to form due to the lateral forces. Hence, the biasing of these forces to the outer rail of the curve leads to severe wear in the flange of the wheel which is mostly in contact with the track. The biased forces may increase transverse loads on the wheels. The wear in the wheel tread is also occurred due to the contact in the second point of the wheel in its flat area (tread). However, due to the decreasing load in this point because of the increasing lateral point, the wear in this area is considerably lower than or negligible with respect to the wheel flange wear (as can be seen in Figure 5). In the following sections, it is showed that although the wheel tread wear is negligible. However, it can move the contact point in the straight line motion of the wagon.

Figure 6 illustrates the history of wheel profile wear of the critical wheel (the first detached wheel for repairing purposes). In Table 3, the wheel flange thickness (Sd) and the wagon's traveled distance for which these profiles occur, are listed. From Figure 6, it can be found that for track with many curves, such as the Southern line of Iran, the wheel flange wear is highly worn in comparison to the wheel tread. From this point of view, the importance of the study on the wheel wear behavior in such railways is emphasized in order to make the necessary anticipations for the safety requirements and also suggestions to improve the maintenance costs. Therefore, the wheel wear behavior of the critical wheel of the wagon is selected for the considerations. In addition, the technique of curve fitting (see section 2) is used to model the wear behavior of the critical wheel.

3. 2. Contact Ellipse and Contact Pressure

In Figure 7, the points obtained from the recorded profiles of the wagon with respect to the wheel flange of the worn profiles are illustrated along with the modeled from the 1st to 5th order of polynomial functions.

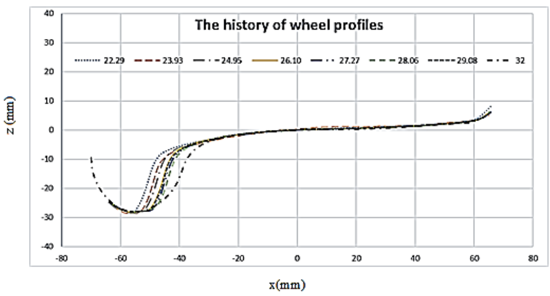

Figure 6. The history of 8 selected profiles from the new standard profile with the Sd=32 mm to the detached worn profile with the Sd=22.29 mm (x and z are the lateral and vertical coordinates)

From the evaluation parameters of fitting denoted in Figure 7, the 5th order polynomial function is appropriate to model the wear behavior of the critical wheel. When the wagon passes through the curves, due to the centrifugal forces, the wagon is biased to one side. The difference in the inner and outer rails' lengths in the curves cause to the sliding of wheel on the outer rail. Therefore, for the rail at the outer side of the curve, the flange of the wheel makes a contact point with the rail in addition to the contact point of wheel tread. Hence, due to the sliding motions and contact points of wheel and rail, the wheel flange is severely worn.

Figures 8 and 9 and Table 3 represent the variation of small and large semi-axis of the contact ellipse and its surface area with respect to the wheel flange thickness (Sd) based on the parameters listed in Table 2.

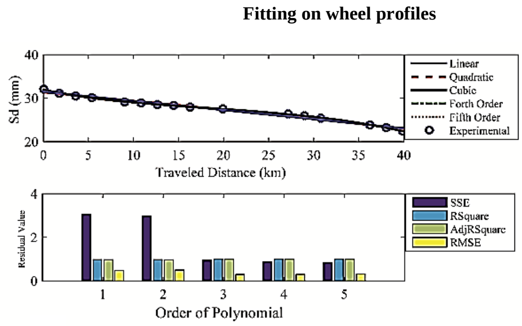

Figure 7. The critical wheel wear behavior from experimental data obtained through field data recording in Southern line of Iran's Railway System

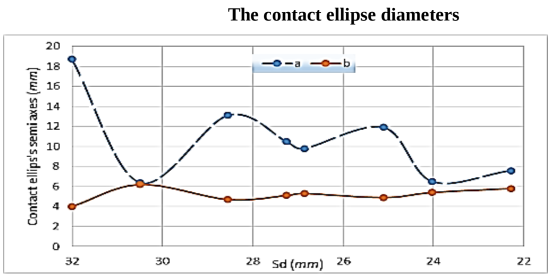

Figure 8. The variation of contact ellipse diameters (*a* and *b*) with respect to the wheel flange thickness (Sd)

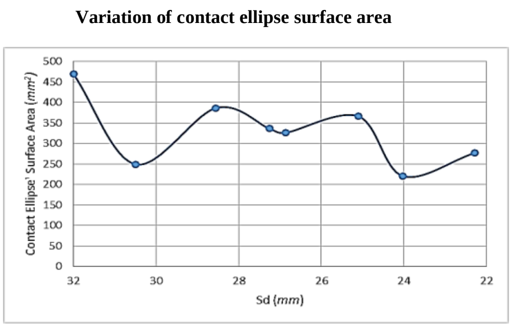

Figure 9. The variation of the contact ellipse's surface area with respect to the wheel flange thickness (Sd)

In Table 3, the parameters such as Sd and traveled distance are experimentally obtained and other parameters such as max pressure, the transverse curvature radius of wheel, and the contact ellipse diameters (*a* and *b*) are calculated through the procedure presented for HCT (Figure 8).

3. 3. Contact Pressure Figure 10 shows the variation of the maximum pressure on the wheel profiles for the travelling wagon in a straight line with respect to the flange thickness (Sd). As mentioned previously, a one point contact is considered which occurs when the wagon travels in a straight line but not when the wagon passing through the curves. This simplifies the analysis to evaluations of the maintenance strategies. Because, the analyzing the wagon passing through curves, leads too many complexities including the sliding of the wheel and the plastic region. It is evident and Figures 9 and 10 show as well that when the contact surface area is maximum, the contact pressure is minimum and vice versa. Moreover, the flange thickness between 25 to 29 mm, shows the lower values through the travel of the wagon which can be suggested as an appropriate range for maintenance purposes.

Figure 11 shows the extrema of the Hertz contact ellipse with respect to the pressure that is obtained from the analysis of the worn profiles of wheels. The minimum and maximum values of pressure are 500.62 and 1069.4 MPa, respectively. In HCT, the value of pressure varies by concentricity ellipses from zero up to the maximum value. Applying the results of pressure in the center of the contact ellipse for all of the profiles, the pressure variations can be considered and the appropriate stress values applying to the maintenance policies can be discussed. The standard maintenance policies for the general railways are detailed in UIC codes [26]. For example, to detaching the worn wheel in order to repair, the value of wheel flange thickness is the main considered criterion. The presented value in the UIC 510-2 code [26] is a general limit for the railways with mostly straight lines. On the other hand, the limit is the minimum limit but not the optimum limit with respect to the maintenance, the costs of wagon detachments, the costs of reprofilings and other related costs when the wagon is detached. Hence, the presentation of wear behavior as well as stress variations along these railways can be used as a criterion to present appropriate suggestions in addition to the satisfactions of UIC code limits.

TABLE 3. The parameters related to the selected profiles of the critical wheel

Sd (*mm*)	Traveled Distance (*km*)	Transverse Curvature Radius of Wheel (*mm*)	Max. Pressure (*MPa*)	*a* (*mm*)	b (mm)	Contact Ellipse's Surface Area (mm^2)
22.29	39820	527.9	849.55	7.6	5.8	276.95
24.03	36200	240.4	1069.4	6.5	5.4	220.53
25.10	30770	357.8	645.60	11.9	4.9	366.36
26.86	27150	417.67	725.63	9.8	5.3	326.34
27.26	19910	385.9	659.99	10.5	5.1	336.45
28.55	14480	358.2	646.97	13.1	4.7	386.84
30.50	3620	796.2	952.26	6.4	6.2	249.31
32.00	0	320	500.62	18.7	4.0	469.97

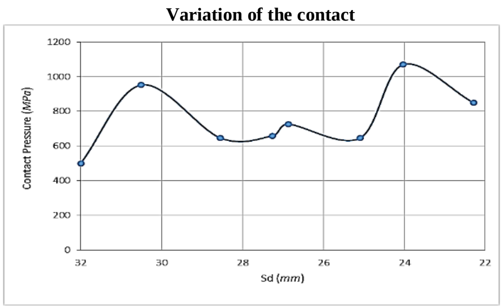

Figure 10. The variation of the contact pressure on the profile of the critical wheel with respect to the wheel flange thickness (Sd)

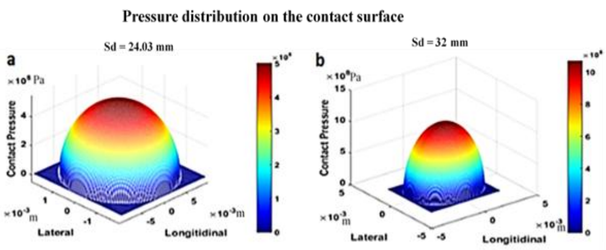

Figure 11. A 3D schematics of the contact ellipse showing the values of pressure on the contact surface for: **(a)** Sd=24.03 mm (Max.) and **(b)** Sd=32 mm (Min.). The maximum pressure occurs at the center of
the ellipse

4. CONCLUSIONS

The experimental results of wheel flange wear on “the Southern line” of Iranian railway, were presented and discussed. The flange thickness limit in which the critical wheel of the wagon was detached, was equal to 22.29 mm. It was found that for the railways with many curves, such as Southern line of Iran, the wheel flange is highly worn. The results showed that the severe wheel flange thickness was occurred due to the biasing of the loadings to the outer rail of the curve.

In addition, the technique of the curve fitting showed that the 5^{th} order polynomial function was appropriate to model the wear behavior of the critical wheel. The wear behavior of two wheels on the critical axis of the wagon showed a higher wear rates for the critical wheel. More wear of the critical wheel causes more contact and more loading on the flange of the wagon wheel.

The contact ellipse’s surface area and pressure are calculated from the evaluated semi-axes *a* and *b*. The minimum and maximum contact ellipse’s surface areas occur in Sd=22.29 and Sd=32 mm, respectively. A one point contact is considered which occurs when the wagon travels in a straight line but not when the wagon passing through the curves. When the contact surface area is maximum, the maximum normal stress shows the minimum values and vice versa. Moreover, the flange thickness region between 25 to 29 *mm*, shows the lower values through the travel of the wagon. According to HCT, the value of pressure varies by concentricity ellipses from zero up to the maximum value. By using the results of maximum normal stress in the center of ellipse for all of the profiles, the pressure variations can be considered as a criterion for the maintenance policies.

5. REFERENCES

1. Zakharov, S., Komarovsky, I. and Zharov, I., "Wheel flange/rail head wear simulation", ***Wear***, Vol. 215, No. 1-2, (1998), 18-24.
2. Kaewunruen, S. and Marich, S., "Severity and growth evaluation of rail corrugations on sharp curves using wheel/rail interaction", in Proceedings of the 20th national convention on civil engineering, (2015).
3. DOURALI, M. and Jalili, M., "Investigation of wagon derailment moving on random rail irregularities using nonlinear 3-dimentional model (research note)", ***International Journal of Engineering, Transactions B: Applications***, Vol. 21, No. 4, (2008), 385-400
4. Telliskivi, T. and Olofsson, U., "Wheel–rail wear simulation", ***Wear***, Vol. 257, No. 11, (2004), 1145-1153.
5. Wang, W.-j., Jiang, W.-j., Wang, H.-y., Liu, Q.-y., Zhu, M.-h. and Jin, X.-s., "Experimental study on the wear and damage behavior of different wheel/rail materials", ***Proceedings of the Institution of Mechanical Engineers, Part F: Journal of Rail and Rapid Transit***, Vol. 230, No. 1, (2016), 3-14.
6. Ekberg, A., Kabo, E., Karttunen, K., Lindqvist, B., Lundén, R., Nordmark, T., Olovsson, J., Salomonsson, O. and Vernersson, T., "Identifying the root causes of damage on the wheels of heavy haul locomotives and its mitigation", ***Proceedings of the Institution of Mechanical Engineers, Part F: Journal of Rail and Rapid Transit***, Vol. 228, No. 6, (2014), 663-672.
7. Clayton, P., "Tribological aspects of wheel-rail contact: A review of recent experimental research", ***Wear***, Vol. 191, No. 1-2, (1996), 170-183.
8. Lewis, R. and Olofsson, U., "Wheel-rail interface handbook, Elsevier, (2009).
9. Enblom, R., "Deterioration mechanisms in the wheel–rail interface with focus on wear prediction: A literature review", ***Vehicle System Dynamics***, Vol. 47, No. 6, (2009), 661-700.
10. Sheinman, E., "Wear of rails. A review of the american press", ***Journal of Friction and Wear***, Vol. 33, No. 4, (2012), 308-314.
11. Nielsen, J.C. and Johansson, A., "Out-of-round railway wheels-a literature survey", ***Proceedings of the Institution of Mechanical Engineers, Part F: Journal of Rail and Rapid Transit***, Vol. 214, No. 2, (2000), 79-91.
12. Zacher, M., Nicklisch, D., Grabner, G., Polach, O. and Eickhoff, B., "A multi-national survey of the contact geometry between wheels and rails", ***Proceedings of the Institution of Mechanical Engineers, Part F: Journal of Rail and Rapid Transit***, Vol. 229, No. 6, (2015), 691-709.
13. Jendel, T., "Prediction of wheel profile wear—comparisons with field measurements", ***Wear***, Vol. 253, No. 1-2, (2002), 89-99.
14. Moreno-Ríos, M., Gallardo-Hernández, E.A., Vite-Torres, M. and Peña-Bautista, A., "Field and laboratory assessments of the friction coefficient at a railhead", ***Proceedings of the Institution of Mechanical Engineers, Part F: Journal of Rail and Rapid Transit***, Vol. 230, No. 1, (2016), 313-320.
15. Ansari, M., Hazrati, I., Esmailzadeh, E. and Azadi, S., "Wear rate estimation of train wheels using dynamic simulations and field measurements", ***Vehicle System Dynamics***, Vol. 46, No. 8, (2008), 739-759.
16. Yan, W. and Fischer, F., "Applicability of the hertz contact theory to rail-wheel contact problems", ***Archive of Applied Mechanics***, Vol. 70, No. 4, (2000), 255-268.
17. Zakharov, S. and Zharov, I., "Simulation of mutual wheel/rail wear", ***Wear***, Vol. 253, No. 1-2, (2002), 100-106.
18. Chen, Y., "The effect of proximity of a rail end in elastic-plastic contact between a wheel and a rail", ***Proceedings of the Institution of Mechanical Engineers, Part F: Journal of Rail and Rapid Transit***, Vol. 217, No. 3, (2003), 189-201.
19. Farris, T., Keer, L. and Steele, R., "Life prediction for unstable shell growth in rails", ***Journal of Engineering for Industry***, Vol. 112, No. 2, (1990), 175-180.
20. Müller, S. and Knothe, K., "Stability of wheelset-track dynamics for high frequencies", ***Archive of Applied Mechanics***, Vol. 67, No. 6, (1997), 353-363.
21. Ekberg, A., Bjarnehed, H. and Lundbéan, R., "A fatigue life model for general rolling contact with application to wheel/rail damage", ***Fatigue & Fracture of Engineering Materials & Structures***, Vol. 18, No. 10, (1995), 1189-1199.
22. Fisette, P. and Samin, J.-C., "A new wheel/rail contact model for independent wheels", ***Archive of Applied Mechanics***, Vol. 64, No. 3, (1994), 180-191.
23. Enblom, R. and Berg, M., "Proposed procedure and trial simulation of rail profile evolution due to uniform wear", ***Proceedings of the Institution of Mechanical Engineers, Part F: Journal of Rail and Rapid Transit***, Vol. 222, No. 1, (2008), 15-25.

24. Aceituno, J.F., Wang, P., Wang, L. and Shabana, A.A., "Influence of rail flexibility in a wheel/rail wear prediction model", ***Proceedings of the Institution of Mechanical Engineers, Part F: Journal of Rail and Rapid Transit***, Vol. 231, No. 1, (2017), 57-74.

25. Huang, L., Li, Z., Li, L. and An, Q., "Methods to calculate accurate wheel/rail contact positions and static contact stress levels", ***Proceedings of the Institution of Mechanical Engineers, Part F: Journal of Rail and Rapid Transit***, Vol. 230, No. 1, (2016), 138-150.

26. Code, U., "510-2. Trailing stock: Wheels and wheelsets", ***Conditions concerning the use of wheels of various diameters. 4th ed. Paris: International Union of Railways***, Vol., No., (2004).

27. Yamashita, S. and Sugiyama, H., "Numerical procedure for dynamic simulation of two-point wheel/rail contact and flange climb derailment of railroad vehicles", ***Journal of Computational and Nonlinear Dynamics***, Vol. 7, No. 4, (2012), 041012.

28. Sebesan, I., Tudorache, C., Dumitriu, M. And Spiroiu, M., "The study of the wheel diameter influence over the loading capacity of a railway vehicle", ***Mechanics***, Vol. 840, No., (2009), 760.

A Study on the Contact Ellipse and the Contact Pressure During the Wheel Wear through Passing the Tracks including Several Sharp Curves

S. M. Salehi, G. H. Farrahi, S. Sohrabpour

School of Mechanical Engineering, Sharif University of Technology, Tehran, Iran

P A P E R I N F O

Paper history:
Received 19 December 2017
Received in revised form 11 February 2018
Accepted 19 February 2018

Keywords:
Wheel Wear
Maintenance Technique
Sharp Curved Railways
Empirical Study
Wheel Flange Wear
Wheel Longevity Enhancement

چکیده

در دهه‌های گذشته،سایش چرخ به عنوان یکی از نگرانی‌ها در حمل‌ونقل ریلی بوده است. مطالعه تغییرشکل تماس‌های چرخ وریل در خطوط خاصیکه شاملپیچ‌های تند هستندبه شناسایی خطرات ناشی ازسایش شدیدیا فاجعه‌بار کمک می‌کند تا هزینه‌های تعمیرونگهداری به منظور رقابتی شدن در کسب و کار حمل‌ونقلبه حداقل برسد. در این مقاله، تماس چرخ و ریل در این مسیرهای خاص مورد مطالعه قرار گرفته است. اندازه‌گیری‌های تجربی پروفیل‌های چرخ به عنوان یک ورودی برایتئوری تماس هرتس (HCT) مورد استفاده قرار گرفته است. یافته‌ها حاکی از آن است که: ۱) برای اینوع خطوط راه‌آهن، سایش زیادی در فلنج چرخ رخ می‌دهد؛ ۲) یک تابع چندجمله‌ایمرتبه ۵ برای مدلسازی رفتار سایشی چرخ بحرانی مناسب است؛ ۳) حداقل و حداکثر مساحت‌های سطح بیضی تماس به ترتیب در ضخامت‌های فلنج ۲۲/۲۹ و ۳۲ میلیمتررخ می‌دهد؛ ٤) حداکثر و حداقل مساحت‌های سطح بیضی تماس در نقاطی که در آن فشار تماس حداقل و حداکثر است رخ می دهد؛ و در نهایت ۵) ناحیه ضخامت فلنج بین ۲۵ تا ۲۹ میلیمتر را می‌توان به عنوان محدوده مناسب برای اهداف تعمیرونگهداری چرخ انتخاب کرد.

***doi**: 10.5829/ije.2018.31.05b.19*